

Stability Analysis for a Flywheel Supported on Magnetic Bearings with Delayed Feedback Control

Ling L. Zhang^{1,2} and Jian H. Huang¹

¹ College of Science
National University of Defense Technology, Changsha, Hunan, 410073, P. R. China
z002005@163.com, jhhuang32@nudt.edu.cn

² Department of Information Technology
Hunan Women's University, Changsha, Hunan, 410004, P. R. China
linglingmath@gmail.com

Abstract — In this paper, the model of the rotor dynamics of the flywheel is given using a rigid rotor supported on magnetic bearings. The phase lag of the control loop is modeled by a simple time delay. Limits of stability and the associated vibration frequencies are described in terms of nondimensional magnetic bearing stiffness and damping and nondimensional parameters of flywheel speed and time delay. Compared to the theoretical values, the simulation results and experimental measurements show the stability boundaries of the PD controller have the same qualitative tendencies.

Index Terms — Flywheel, magnetic bearing, PD controller, stability, time delay.

I. INTRODUCTION

As a new type of attitude control actuator of spacecraft, the magnetic levitation flywheel has many advantages such as no friction, high energy density, long life capability for up to 90 percent depth of discharge, peaking or pulse power capability and so on. Flywheels can be also an alternative to batteries and reaction wheels for the space system. Therefore magnetic levitation flywheel is an important direction of space technology development.

Since 1960's, developed countries have begun to work on the magnetic levitation flywheel [1-4]. After decades of development, the magnetic suspension flywheel technology have made great progress in the magnetic bearing structure design and optimization, the dynamics and mechanics analysis, modeling and model identification, control method, high performance sensors and power amplifier and so on; but there are still many technical difficulties. The vibration suppression control of maglev flywheel is a key to display the maglev flywheel space applications such as low loss, high precision, long life and other advantages [5].

The magnetic bearing system uses magnetic forces

to levitate the shaft between opposing magnetic poles. The rotor is attracted to one pole or the other pole and is inherently unstable, then the magnetic bearing system of a flywheel is stabilized with an active control system. In the process of eddy current proximity sensors, anti-alias filters, digital controller, re-construction filter, power amplifier, the magnetic bearing forces, each of the components involved in the magnetic bearing and control system has a time delay associated with the components. The total time delay is the sum of the individual time delays [6]. Time-delayed systems, which have been studied for various applications and control systems, may admit rich dynamics, including bifurcations and chaotic motions [7-11]. Hosek [12] developed a single-step automatic tuning algorithm as a means of increasing robustness against uncertainties and variations in the mechanical properties of the absorber arrangement. In studying the stability robustness of systems with multiple independent and uncertain delays, Fazelinia [13, 14] used the building hypersurfaces to arrive at the complete stability robustness picture in the domain of the delays. In recent years, some scholars began to study the characteristics of magnetic suspension flywheel from a dynamics behavior aspect, thus providing theoretical guidance to suppress vibration [15-19]. Based on decentralized PD controller, Polajzer [15] and Kascak [6] established the coupled dynamics model for the active magnetic bearing and analyzed the rotor critical speed using the Hopf bifurcation theory; Zhang [16] studied the global bifurcation and chaotic vibration for time-varying stiffness of the magnetic bearing, and discussed the bifurcation of the average equation using the normal form theory. Zhang [17] derived the averaged equation using the perturbation analysis method, then studied the transient and steady-state vibration response of the nonlinear magnetic bearing with the numerical simulation method. In these above research, only a few papers consider the effect of the time delay on the

stability of the magnetic flywheel.

According to the details of the flywheel mechanical design and the performance requirements, many different approaches have been used, varying from PID to modal or adaptive methods [20]. For example, Pichot [21] discussed the benefits of a notch filter based controller in comparison to a PID control for a large flywheel. Palazollo [22] developed a modal control system which was applied to a 60,000 rpm flywheel. In this paper, we will use a P-D controller which causes the magnetic bearing to produce two forces: one is proportional to the displacement and the other is proportional to the derivative of the displacement, the velocity.

This paper theoretically describes the stability boundaries of the magnetic bearing controller which levitates the high speed flywheel rotor. In Section 2, based on current stiffness and displacement stiffness of magnetic bearing, linear motion differential equation for maglev flywheel is established. Section 3 analyzes the stability limits and the associated vibration frequencies about two variables of these system parameters and control parameters. We give the simulation and experiment results in Section 4 and compare them to the theoretical values. Finally, the main conclusions drawn in this paper are summarized in Section 5.

II. FLYWHEEL STABILITY ANALYSIS

Figure 1 shows the rotor displacement of magnetic suspension flywheel with four axes and lateral axis of a flywheel [23]. The magnetic bearing sensors $s_1 - s_4$ are installed on the forward whirl and $s_5 - s_8$ on the backward whirl, and the distance of the up and down sensor planes is l . The magnetic bearing axis is OZ and the direction of radial axis points to the sensor measurement point. From Fig. 1, the displacement signals of the rotor $u_1 - u_8$ are measured by the eight sensor measurement points of the magnetic suspension flywheel with four axes. By the differential process, we can get the displacement signals of the flywheel rotor x_1, x_2, y_1 and y_2 , as follows:

$$x_1 = \frac{u_1 - u_3}{k_s}, \quad y_1 = \frac{u_2 - u_4}{k_s},$$

$$x_2 = \frac{u_5 - u_7}{k_s}, \quad y_2 = \frac{u_8 - u_6}{k_s},$$

where k_s represents the sensor gain.

Denote the displacement of the center of mass by x and y , then,

$$x = \frac{x_1 + x_2}{2}, \quad y = \frac{y_1 + y_2}{2}.$$

Denote the angles motion of the center of mass about X and Y axes respectively:

$$\alpha = \frac{y_2 - y_1}{l}, \quad \beta = \frac{x_2 - x_1}{l}.$$

In the definition of the angles, we use the upper plane parameters minus the under plane parameters, therefore β denotes the positive direction along the Y axis and α represents the negative direction along the X axis.

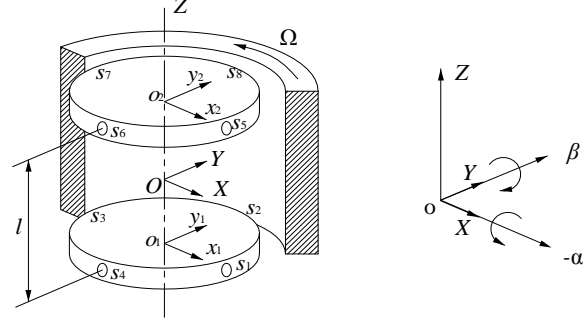


Fig. 1. The rotor displacement of magnetic suspension flywheel with four axes and lateral axis of a flywheel.

The control currents i_1, i_2, i_3, i_4 are applied to the port voltage of the electromagnet according to these four position signals, the induced forces are:

$$F_{x1} = k_x x_1 + k_i i_1, \quad F_{x2} = k_x x_2 + k_i i_2, \quad (1)$$

$$F_{y1} = k_x y_1 + k_i i_3, \quad F_{y2} = k_x y_2 + k_i i_4, \quad (2)$$

where k_x and k_i represent the control gains of the displacement and the current respectively.

The rotor dynamics of the flywheel can be described in terms of the motion of the center of mass and rotations about the center of mass. For small displacements the lateral motion is uncoupled from the axial motion. The lateral equations of motion of the center of mass are:

$$\frac{m}{2}(\ddot{x}_1 + \ddot{x}_2) = k_x x_1 + k_i i_1 + k_x x_2 + k_i i_2, \quad (3)$$

$$\frac{m}{2}(\ddot{y}_1 + \ddot{y}_2) = k_x y_1 + k_i i_3 + k_x y_2 + k_i i_4, \quad (4)$$

where m is the mass of the flywheel rotor.

For small rotations, the equations of angular motion about the center of mass are:

$$J_d \ddot{\alpha} + J_p \Omega \dot{\beta} = \frac{l}{2} [(k_x y_2 + k_i i_4) - (k_x y_1 + k_i i_3)], \quad (5)$$

$$J_d \ddot{\beta} - J_p \Omega \dot{\alpha} = \frac{l}{2} [(k_x x_2 + k_i i_2) - (k_x x_1 + k_i i_1)], \quad (6)$$

where Ω is a circular frequency of the flywheel, J_d and J_p are the transverse and polar moments of inertia respectively. $J_p \Omega \dot{\alpha}$ and $J_p \Omega \dot{\beta}$ are the gyro items.

Using P-D controller, the control currents are as follows:

$$i_1 = k_p x_1 + k_d \dot{x}_1, \quad i_2 = k_p x_2 + k_d \dot{x}_2, \quad (7)$$

$$i_3 = k_p y_1 + k_d \dot{y}_1, \quad i_4 = k_p y_2 + k_d \dot{y}_2, \quad (8)$$

where k_p and k_d are proportional and derivative feed-

back control gains respectively. Combining Equations (3)-(8), we have:

$$\frac{m}{2}(\ddot{x}_1 + \ddot{x}_2) = (k_x + k_i k_p)(x_1 + x_2) + k_i k_d(\dot{x}_1 + \dot{x}_2), \quad (9)$$

$$\frac{m}{2}(\ddot{y}_1 + \ddot{y}_2) = (k_x + k_i k_p)(y_1 + y_2) + k_i k_d(\dot{y}_1 + \dot{y}_2), \quad (10)$$

$$J_d \ddot{\alpha} + J_p \Omega \dot{\beta} = \frac{l^2}{2}(k_x + k_i k_p)\alpha + \frac{l^2}{2}k_i k_d \dot{\alpha}, \quad (11)$$

$$J_d \ddot{\beta} - J_p \Omega \dot{\alpha} = \frac{l^2}{2}(k_x + k_i k_p)\beta + \frac{l^2}{2}k_i k_d \dot{\beta}. \quad (12)$$

The solution for the motion of the center of mass and that for the rotation about the center of mass is of the same form, if the shaft speed Ω is set equal to zero [24, 25]. Therefore only motion of the rotation about the center of mass will be solved. The classical small signal stability analysis assumes an eigenvalue solution of the equation of motion.

A centralized controller decouples the motion of the center of mass and the rotation about the center of mass. The controller terms have a time delay associated with the various components in the control loop. Let $x(t) = [\alpha, \dot{\alpha}, \beta, \dot{\beta}]^T$, and the equations of motion become:

$$\dot{x}(t) = Px(t) + Qx(t - \tau), \quad (13)$$

where

$$P = \begin{pmatrix} 0 & 1 & 0 & 0 \\ \frac{l^2 k_x}{2J_d} & 0 & 0 & -\frac{J_p \Omega}{J_d} \\ 0 & 0 & 0 & 1 \\ 0 & \frac{J_p \Omega}{J_d} & \frac{l^2 k_x}{2J_d} & 0 \end{pmatrix}, Q = \begin{pmatrix} 0 & 0 & 0 & 0 \\ \frac{l^2 k_i k_p}{2J_d} & \frac{l^2 k_i k_d}{2J_d} & 0 & 0 \\ 0 & 0 & 0 & 0 \\ 0 & 0 & \frac{l^2 k_i k_p}{2J_d} & \frac{l^2 k_i k_d}{2J_d} \end{pmatrix}.$$

If the characteristic solution is assumed to be:

$$x(t) = Ae^{\lambda t}.$$

We only consider the first term of the corresponding characteristic Equation of (13):

$$J_d \lambda^2 - i\Omega J_p \lambda - \frac{l^2}{2}k_i k_d \lambda e^{-\lambda \tau} - \frac{l^2}{2}k_i k_p e^{-\lambda \tau} - \frac{l^2}{2}k_x = 0. \quad (14)$$

The characteristic equation does not have a real solution unless Ω is zero. If the eigenvalue is complex, let $\lambda = \mu + i\omega$. The vibrations grow in time and the system is unstable with $\mu > 0$ and the vibrations decay in time and the system is stable with $\mu < 0$. $\mu = 0$ defines the stability boundary. Substituting $\lambda = i\omega$ into [14] and separating the real and imaginary parts of [14], we obtain:

$$\begin{aligned} -J_d \omega^2 + \Omega J_p \omega - \frac{l^2}{2}k_x - \frac{l^2}{2}k_i k_p \cos \omega \tau - \frac{l^2}{2}k_i k_d \omega \sin \omega \tau &= 0 \\ \frac{l^2}{2}k_i k_p \sin \omega \tau - \frac{l^2}{2}k_i k_d \omega \cos \omega \tau &= 0. \end{aligned}$$

From the above imaginary and the real parts equations respectively, we can get the expression of τ

and Ω , that is Equations (15) and (16). By means of solving the real and the imaginary parts equations group, we would get the expressions of the control parameters k_p and k_d ((17) and (18)):

$$\tau = \frac{1}{\omega} \arctan \frac{k_d \omega}{k_p} + k\pi, k = 0, 1, 2, 3, \dots, \quad (15)$$

$$\Omega = \frac{1}{J_p \omega} (J_d \omega^2 + \frac{l^2}{2}(k_x + k_i(k_p \cos \omega \tau + k_d \omega \sin \omega \tau))), \quad (16)$$

$$k_p = -\frac{2}{l^2 k_i} \sqrt{(J_d \omega^2 - \Omega J_p \omega + \frac{l^2}{2}k_x)^2 - (\frac{l^2}{2}k_i k_d \omega)^2}, \quad (17)$$

$$k_d = -\frac{2}{l^2 k_i \omega} \sqrt{(J_d \omega^2 - \Omega J_p \omega + \frac{l^2}{2}k_x)^2 - (\frac{l^2}{2}k_i k_p)^2}. \quad (18)$$

Combing (15) with another one of (16), (17) and (18), we can get the stability boundary. For example, Equations (15) and (16) define the non-dimensional flywheel speed and the time delay at the transition between stable and unstable operation of the flywheel; Equations (15) and (17) describe curves in the k_p, τ parameter space which are parameterized by ω . Similarly, we can get any two variables from the transformation of the real part and the image part equations, for example,

$$k_d = \frac{2 \sin \omega \tau}{l^2 k_i \omega} (-J_d \omega^2 + \Omega J_p \omega - \frac{l^2}{2}k_x), k_p = k_d \omega \cot \omega \tau. \quad (19)$$

From (19), we can get the stability boundary for the flywheel in the k_p, k_d parameters space.

We will illustrate these results with two examples. The realistic values for the physical parameters are given in Table 1. For magnetic suspension flywheel system, the gyro effect is very small when the rotor is static or rotates at low speed. Therefore by dividing into four single degree of freedom, the appropriate stiffness and damping can make the rotor suspend stably in this case. In this paper, the rotate speed is about 20π rad/s, which is below the critical value, and then the effect of the rotor is omitted.

Table 1: Physical parameter values

J_d	J_p	m	l	k_i	k_x	k_s
0.01kg·m ²	0.02kg·m ²	4kg	0.016m	-150N/A	650000N/m	8000V/m

Case (1)

With the proportional gain $k_p = 0.7$ and the shaft speed $\Omega = 20\pi$, we use (15) and (18) with $k = 0$ to plot the time delay τ and the derivative gain k_d as ω is varied (Fig. 2). We do not show the curves with $k > 0$ as they all lie on the right of the corresponding curve with $k = 0$, and hence, do not form part of the stability boundary.

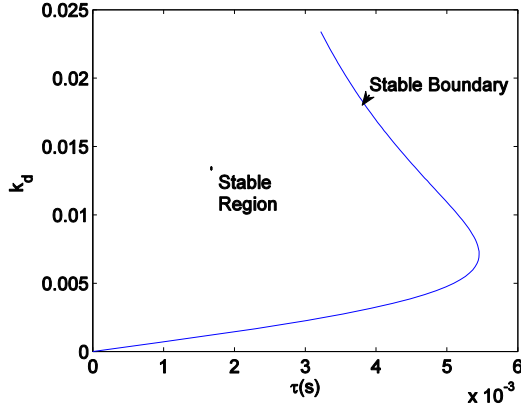


Fig. 2. The correlation of stability limits of a flywheel supported on magnetic bearings with time delay for $k_p = 0.7$, $\Omega = 20\pi$.

Case (2)

With the time delay $\tau = 0.001s$ and the shaft speed $\Omega = 20\pi$, we use (17) and (18) to plot the proportional gain k_p and the derivative gain k_d as ω is varied. Figure 3 shows both the static and dynamic stability for a magnetic flywheel with time delay. The proportional gain k_p for the static stability analysis is given by (14) with $\lambda = 0$. For both the static and dynamic stability analysis, if the real part of the eigenvalue μ is defined positive, the vibrations grow in time and the system is unstable. If μ is negative, the vibration will decay in time and the flywheel system is stable. $\mu = 0$ defines the stability boundary.

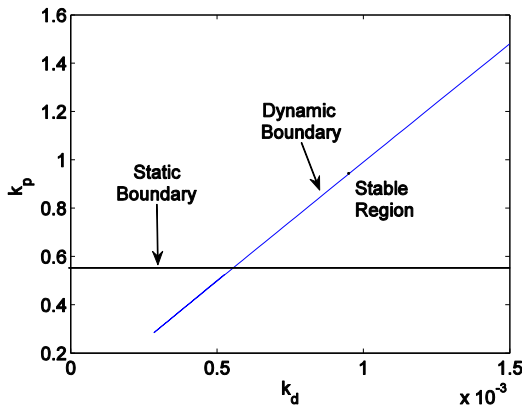


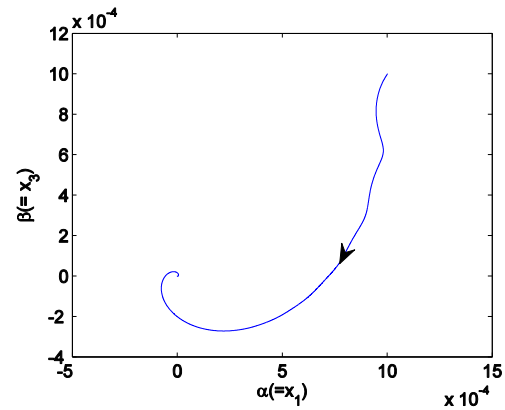
Fig. 3. The correlation of stability limits frequency of a flywheel supported on magnetic bearings with time delay for $\tau = 0.001s$, $\Omega = 20\pi$.

III. NUMERICAL SIMULATIONS

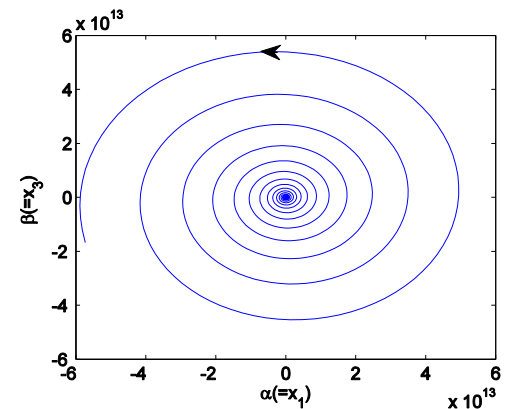
In this section, we consider the flywheel system (11)-(12) with the physical parameters given in Table 1.

According to the two examples in Section II (Fig. 2 and Fig. 3), we will compare these theoretical results with numerical simulations of the system (11)-(12). Using the DDE Toolbox for Matlab, we can get the numerical solutions for the angular motions α, β of the center of mass about X and Y axes and draw their trajectory.

Together with (15) and (18), if the time delay and the derivative gain change, we will study the stability of the flywheel system with $k_p = 0.7$, $\Omega = 20\pi$. Choosing the point $(\tau, k_d) = (0.004, 0.01)$ which lies in the stable region of Fig. 2, from Fig. 4 (a), the angular motions α, β of the center of mass about X and Y axes approach the trivial solution, indicating that it is asymptotically stable. Then we adjust the parameter k_d as 0.02 and the time delay τ remains the same, that is the point $(\tau, k_d) = (0.004, 0.02)$ is out of the stable region of Fig. 2, the values of α, β grow quickly, which suggests that the flywheel system is unstable from Fig. 4 (b). If the derivative gain $k_d = 0.02$ remains unchanged and the time delay changes as $\tau = 0.003s$, that is the point $(\tau, k_d) = (0.003, 0.02)$ lies in the stable region of Fig. 2 again, the flywheel system will restore to the stable operation from Fig. 4 (c).



(a) $\tau = 0.004s$, $k_d = 0.01$



(b) $\tau = 0.004s$, $k_d = 0.02$

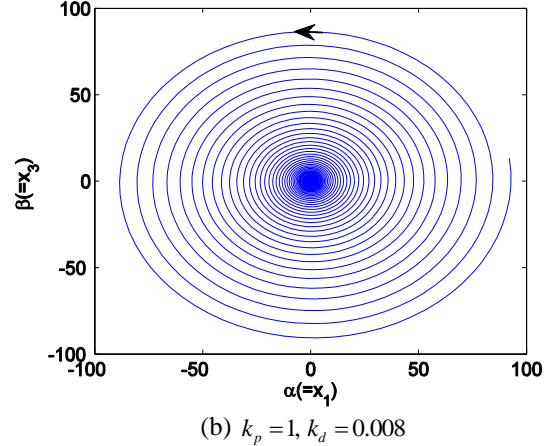
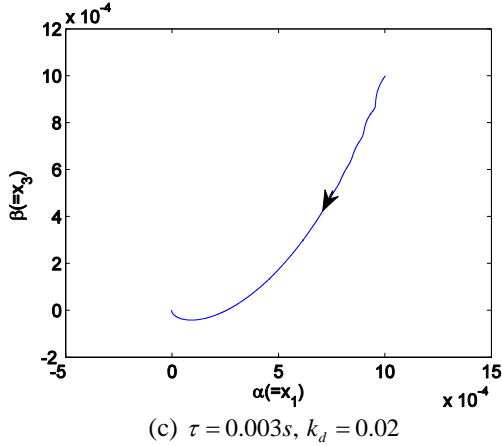


Fig. 4. Numerical simulations of the maglev flywheel system (13), τ and k_d as indicated. (a), (b), and (c) are (pseudo) phase portraits of the angular motions (α and β) of the center of mass about X and Y axes.

In another example of Section II, with (19), $\tau = 0.001s, \Omega = 20\pi$. Choosing the point $(k_p, k_d) = (1, 0.02)$ which lies in the stable region of Fig. 3, from Fig. 5 (a), the angular motions α, β of the center of mass about X and Y axes approach the trivial solution, indicating that the equilibrium point is stable. Then we adjust the parameter k_p as 0.008 and the derivative gain k_d remains unchanged, that is the point $(k_p, k_d) = (1, 0.008)$ is out of the stable region of Fig. 3, the values of α, β grow rapidly, which suggests that the flywheel system loses the stability from Fig. 5 (b). If the derivative gain $k_d = 0.008$ remains the same, the proportional gain changes as $k_p = 0.6$, that is the point $(k_p, k_d) = (0.6, 0.008)$ lies in the stable region of Fig. 3 again, the flywheel system will restore the stability from Fig. 5 (c).

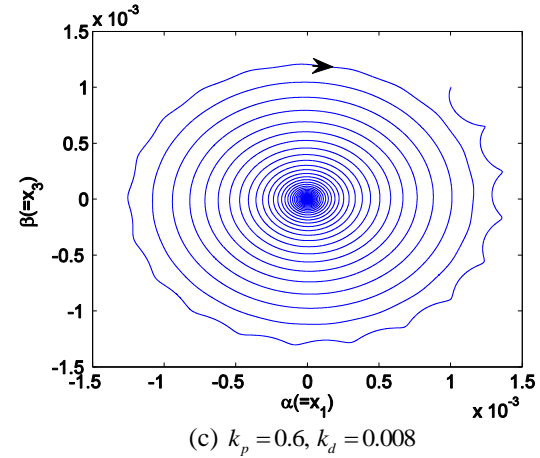
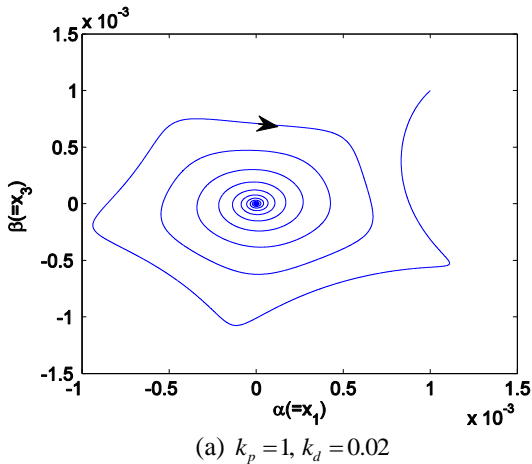


Fig. 5. Numerical simulations of the maglev flywheel system (13). k_p and k_d as indicated. (a), (b), and (c) are (pseudo) phase portraits of the angular motions (α and β) of the center of mass about X and Y axes.

Thus, the numerical simulations agree with the stable boundary diagrams of Figs. 2, 3 as predicted by the theory. When the values of the time delay, the shaft speed and the control parameters fall in the stable region (Fig. 2 and Fig. 3), the numerical solutions for the magnetic flywheel system will tend to be stable (Figs. 4 (a), (c) and Figs. 5 (a), (c)). If these values in the unstable region, the numerical solutions for the magnetic flywheel system will lose their stability (Fig. 4 (b) and Fig. 5 (b)). These results suggest that the magnetic flywheel will remain stable in the experiment and practical application by choosing the appropriate parameters values according the theoretical results.

IV. EXPERIMENT

Test was performed in Changsha. We will use the physical parameters given in Table 1 and choose $k_p = 0.07, \Omega = 20\pi$.

For a given time delay, the derivative gain is varied noting the region of stable operation. The measured result for the forward whirl is shown as Fig. 6 (a), which describes the correlation of stability data of the forward whirl shown on Fig. 2. The region of stable operation is limited at small time delay by the derivative gain. That is, there is no stable region of operation if the time delay at a high value. Then using $\tau = 0.001$, $\Omega = 20\pi$, for a given derivative gain, the proportional gain is varied noting the region of stable operation. The measured result Fig. 6 (b) shows the correlation of stability data of the forward whirl shown on Fig. 3. There is no stable region of operation if the proportional gain at a low value. The measured result for the forward whirl is shown in Fig. 6. The experiment results have the similar shaped regions of stability compared to the theoretical simulation.

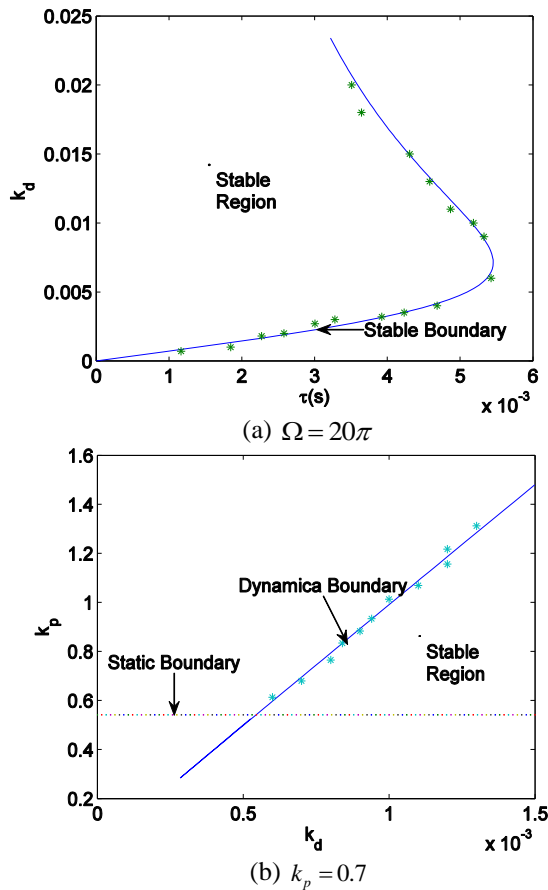


Fig. 6. The measured result for the forward whirl compared to the theoretical simulation.

We have tried different pairs of k_p and Ω and the shapes of the curves defined by (15) and (18) and their behaviors as k_p and Ω are varied are similar to what is shown in Fig. 7. Figure 7 (a) shows the stability region

for Ω fixed and varying k_p . Increasing the value of k_p decreases the size of the stability region. Figure 7 (b) shows the stability region for k_p fixed and varying Ω . Increasing Ω decreases the size of the stability region.

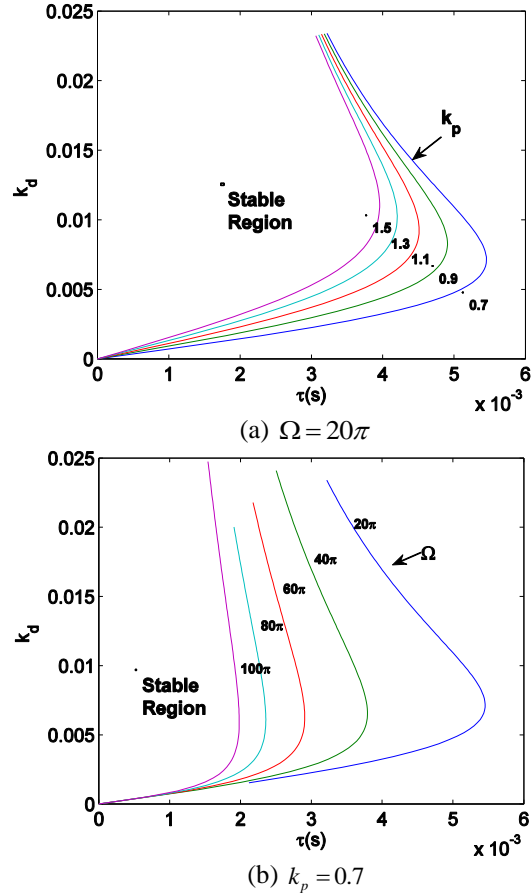


Fig.7. The stability map for a flywheel supported on magnetic bearings with time delay for various values of the proportional gain k_p or the shaft speed Ω .

Note that in all cases, the range of values of k_d for which the flywheel system is stable decreases as τ increases and there is a critical value of τ , τ_c , such that the equilibrium point is unstable for any k_d if $\tau > \tau_c$, where τ_c is the τ value at the maximum.

V. CONCLUSIONS

In this paper, the stability boundaries of the suspension system of a magnetic flywheel with time-delayed proportional, derivative feedback are studied.

According to the characteristic equation of the flywheel system, we get the stable region in the any two parameters spaces of τ, Ω, k_p, k_d . For example, a set of values of the time delay and the derivative feedback gain

for which the flywheel system is stable can then be described. For the parameter values that we investigated, the larger the proportional gain, the smaller the region of the stability; the larger the shaft speed, the smaller the region of the stability. At the same time, we should also control the time delay of the system, if the time delay larger than the critical value, the equilibrium position is unstable for any derivative gain. Numerical simulations of the full model confirmed the predictions of the analysis. Experimental measurements showed that the results of the modeling have the same qualitative tendencies as theoretical analysis.

To completely understand the dynamic behavior of the flywheel system, further research needs be carried out. Although the magnetic flywheel has the similar magnetic bearing system with the magnetic train [26, 27], but the principle of the flywheel is more complicated for considering the motion of the center mass and rotations about the center of mass. In the next step, with DR (delayed resonator) and CTCR (Cluster Treatment of Characteristic Roots) [12-14], we will carry up a more detailed stability treatment of delayed flywheel system to increase robustness against uncertainties and variations. Therefore it would be interesting to extend the dynamical behaviors research of the flywheel system such as Hopf bifurcation, chaotic behavior and so on.

ACKNOWLEDGMENT

This work was supported by National Natural Science Foundation of China (11301173) and Natural Science Foundation of Hunan Province (14JJ3143), Scientific Research Key Project of Hunan Provincial Education Department (16A106) and China Postdoctoral Science Foundation (2014M562651, 2016T90977).

REFERENCES

- [1] P. Poubeau, *Satellite momentum wheel*, United States Patent: 3955858, May 1976.
- [2] S. Michael, R. Thomas, and B. Enrico, "The challenges of miniaturisation for a magnetic bearing wheel," *Proceedings of 9th European Space Mechanisms and Tribology Symposium*, Liege, Belgium, pp. 17-24, Sep. 2001.
- [3] G. Bernd, E. Markus, and K. R. Hans, "Gimballing magnetic bearing reaction wheel with digital controller," *Proceedings of the 11th European Space Mechanisms and Tribology Symposium*, Lucerne, Switzerland, pp. 1-6, Sep. 2005.
- [4] B. C. Han, "Modeling and analysis of novel integrated radial hybrid magnetic bearing for magnetic bearing reaction wheel," *Chinese Journal of Mechanical Engineering*, vol. 23, pp. 655-662, Nov. 2010.
- [5] L. Y. Xiang, S. G. Zuo, and L. C. He, "Electric vehicles to reduce vibration caused by the radial force," *The Applied Computational Electromagnetics Society*, vol. 29, pp. 340-350, Sep. 2014.
- [6] A. F. Kacsak, G. V. Brown, and Q. H. Jansen, "Stability limits of a PD controller for a flywheel supported on rigid rotor and magnetic bearings," *AIAA Guidance, Navigation and Control Conference and Exhibition*, San Francisco, California, pp. 5956, Aug. 2005.
- [7] J. Wu, *Theory and Applications of Partial Functional Differential Equations*. Springer, New York, 1996.
- [8] S. Guo, Y. Chen, and J. Wu, "Two-parameter bifurcations in a network of two neurons with multiple delays," *J. Differential Equations*, vol. 244, pp. 444-486, Jan. 2008.
- [9] B. Hassard, N. Kazarinoff, and Y. Wan, *Theory and Applications of Hopf Bifurcation*. Cambridge University Press, Cambridge, 1981.
- [10] O. M. Ramahi, "Analysis of conventional and novel delay lines: A numerical study," *The Applied Computational Electromagnetics Society*, vol. 18, pp. 181-190, Aug. 2003.
- [11] P. Orlov, T. Gazizov, and A. Zabolotsky, "Short pulse propagation along microstrip meander delay lines with design constraints: Comparative analysis of the quasi-static and electromagnetic approaches," *The Applied Computational Electromagnetics Society*, vol. 31, pp. 238-243, Mar. 2016.
- [12] M. Hosek and N. Olgac, "A single-step automatic tuning algorithm for the delayed resonator vibration absorber," *IEEE Transactions on Mechatronics*, vol. 7, pp. 245-255, July 2002.
- [13] H. Fazelinia, R. Sipahi, and N. Olgac, "Stability analysis of multiple time delayed systems using 'building block' concept," *Proceeding of the 2006 American Control Conference*, Minnesota, USA pp. 2393-2398, 2006.
- [14] H. Fazelinia, R. Sipahi, and N. Olgac, "Stability robustness analysis of multiple time-delayed systems using 'building block' concept," *IEEE Transactions on Automatic Control*, vol. 52, pp. 799-810, May 2007.
- [15] B. Polajzer, J. Ritonja, and G. Stumberger, "Decentralized PI/PD position control for active magnetic bearings," *Electrical Engineering*, vol. 89, pp. 53-59, Oct. 2006.
- [16] W. Zhang, J. W. Zu, and F. X. Wang, "Global bifurcations and chaos for a rotor-active magnetic bearing system with time-varying stiffness," *Chaos Solitons & Fractals*, vol. 35, pp. 586-608, May 2008.
- [17] W. Zhang and J. W. Zu, "Transient and steady nonlinear for a rotor-active magnetic bearing system with time-varying stiffness," *Chaos Solitons & Fractals*, vol. 38, pp. 1152-1167, Feb. 2008.

- [18] M. P. Aghababa and H. P. Aghababa, "Chaos suppression of rotational machine systems via finite-time control method," *Nonlinear Dynamics*, vol. 69, pp. 1881-1888, Apr. 2012.
- [19] H. C. Gui, L. Jin, and S. J. Xu, "On the attitude stabilization of a rigid spacecraft using two skew control moment gyros," *Nonlinear Dynamics*, vol. 79, pp. 2079-2097, Mar. 2015.
- [20] Z. W. Liu, R. S. Chen, and J. Q. Chen, "Using adaptive cross approximation for efficient calculation of monostatic scattering with multiple incident angles," *The Applied Computational Electromagnetics Society*, vol. 26, pp. 325-333, Apr. 2011.
- [21] M. A. Pichot, J. P. Kajs, and J. P. Murhy, "Active magnetic bearings for energy storage systems for combat vehicles," *IEEE Transactions on Magnetics*, vol. 37, pp. 318-323, Jan. 2001.
- [22] A. Palazzolo, *System and methods for controlling suspension using a magnetic field*, U.S. Patent: 6323614B1, 2001.
- [23] X. F. Chen, *Research on vibration analysis and inhibitory control of magnetic suspension flywheel system*, Ph.D., National University of Defense Technology, 2011.
- [24] H. W. Wang and J. Q. Liu, "Stability and bifurcation analysis in a magnetic bearing system with time delays," *Chaos, Solitons & Fractals*, vol. 26, pp. 813-825, Mar. 2005.
- [25] J. C. Ji, "Stability and Hopf bifurcation of a magnetic bearing system with time delays," *Journal of Sound and Vibration*, vol. 259, pp. 845-856, Apr. 2003.
- [26] L. L. Zhang, S. A. Campbell, and L. H. Huang, "Nonlinear analysis of a maglev system with time-delayed feedback control," *Physica D*, vol. 240, pp. 1761-1770, July 2011.
- [27] L. L. Zhang, Z. Z. Zhang, and L. H. Huang, "Double Hopf bifurcation of time-delayed feedback control for maglev system," *Nonlinear Dynamics*, vol. 69, pp. 961-967, Mar. 2012.



Ling-Ling Zhang was born in 1982. She received the M.Sc. and Ph.D. degrees in Mathematics from Hunan University, China, in 2007 and 2010, respectively. She is a Postdoctoral Fellow from 2014 to 2017 in College of Science from National University of Defense Technology. She is currently an Associated Professor of Hunan Women's University. Her research interest is the stability and control of maglev system.



Jian-Hua Huang was born in 1968. He received the M.Sc. and Ph.D. degrees in Mathematics from Central China Normal University, China, in 1996 and 2002, respectively. He is currently a Professor of National University of Defense Technology. His main research interests are random dynamical systems and infinite dimensional dynamical systems.